

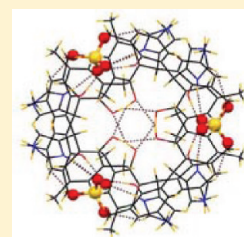
# An Imidazole-Based Bisphenol 2-((2-Hydroxy-3,5-dimethylphenyl)(imidazol-4-yl)methyl)-4,6-dimethylphenol: A Versatile Host for Anions

Bhaskar Nath and Jubaraj B. Baruah\*

Department of Chemistry, Indian Institute of Technology Guwahati, Guwahati – 781039, Assam, India

## S Supporting Information

**ABSTRACT:** Imidazole containing bisphenol 2-((2-hydroxy-3,5-dimethylphenyl)(imidazol-4-yl)-methyl)-4,6-dimethylphenol (**1**), (abbreviated as Imbp) and its salts with dicarboxylic acids and mineral acids, namely, maleic acid (H<sub>2</sub>mal), fumaric acid (H<sub>2</sub>fum), adipic acid (H<sub>2</sub>adpt), perchloric acid, sulphuric acid (sulfate and bisulphate), tetrafluoroboric acid, and nitric acid are structurally characterized. The crystal packing in the solid state structures of the salts are assisted by electrostatic N<sup>+</sup>–H···O and related weak interactions. The bisphenol **1** and its methanol solvate have extensive hydrogen bonded structures; in the later case the methanol molecule acts as a bridge through N–H···O and O–H···O interactions and strong  $\pi\cdots\pi$  interactions between the two imidazole rings. Both the structures have strong intramolecular O–H···O hydrogen bonds among the hydroxyl groups of the Imbp molecule. The mono-deprotonated salts of **1** with maleic acid, adipic acid, have layered structure, whereas anion encapsulation takes place in the case of dideprotonated salts of fumaric acid. In the case of perchlorate, bisulphate, tetrafluoroborate, and nitrate salts of **1** the intramolecular O–H···O is retained. The sulfate anchors trimeric self-assemblies formed through R<sub>3</sub><sup>3</sup> (6) type of hydrogen bond in the protonated **1** and finally they form circular structures with a diameter of 15.193 Å, in which anion is embedded. A bisulphate salt of **1** is prepared by the reaction of magnesium sulfate with sulphuric acid in methanol in the presence of **1**; in this structure bisulphate occurs in pairs through intermolecular hydrogen bonds and it assists in the formation of an assembled structure of the protonated bisphenol **1**.



## INTRODUCTION

Host–guest compounds, also known as inclusion compounds, are a class of compounds where the host framework provides apposite geometry to accommodate guest molecule(s), which include cations, anions, and neutral molecules.<sup>1,2</sup> The rational design of such molecular solids has received significant attention of the crystal engineers because of their potential applications in molecular recognition, separation technology, and heterogeneous catalysis.<sup>3,4</sup> Phenolic compounds such as bisphenols and related compounds are well-known for their ability to form inclusion compounds, and they have found potential applications in molecular recognition.<sup>5–7</sup> Bisphenols are organic compounds having propeller-like geometry, in which the phenolic hydroxyl groups play a critical role to build diverse supramolecular networks such as rings, linear chains, ladders, etc.<sup>8</sup> Two phenolic hydroxy groups provide directional H-bonding sites for the formation of these types of structures.<sup>9</sup> Different types of bisphenol molecules have been reported where the two phenol rings were attached by various spacers. In the majority of the cases, the methylene group is used to connect the two phenol rings.<sup>10</sup> Recently, some bisphenols have been reported, where the two phenol rings are connected by an adamantane spacer.<sup>11</sup> Although there are many literature reports available on the self-assembly and host–guest chemistry of bisphenols, there are only a few references found on heteroatom containing bisphenols. Generally, bisphenols and their related phenolic compounds possess O–H···O and O–H··· $\pi$  (aromatic) interactions in the solid state.<sup>12</sup> The presence

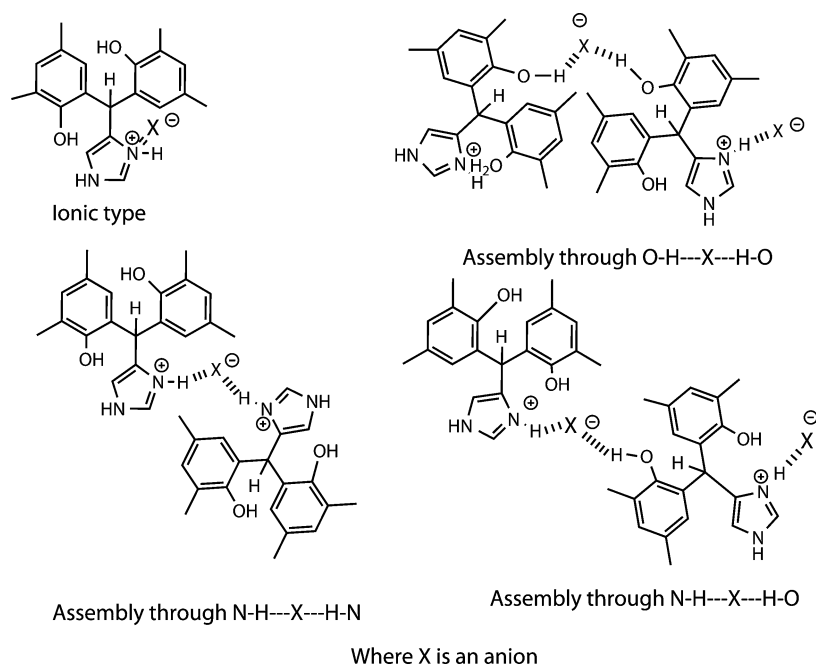
of one or multiple electronegative heteroatom(s) such as nitrogen in any of the ring of bisphenols would introduce additional interactions leading to new supramolecular architectures. Furthermore, such heteroatoms may interact with various anions to give rise to new charge assisted assembly of bisphenols. Pyridine containing bisphenols are used to stabilize methyl and ethyl sulfate salts of pyridinium bisphenols.<sup>13</sup> Heterocycles such as imidazole derivatives are attractive due to their ability to form supramolecular isomers and solvatopolymorphs.<sup>14</sup> Thus, it would be interesting to attach an imidazole unit to bisphenol to make interesting self-assembled structures. Various imidazolium cations that are readily formed on acid treatment of imidazole derivatives generally self-assemble through N–H···N interactions.<sup>15</sup> With these anticipations to construct new charge-assisted assemblies of imidazole containing bisphenols, such as the few possibilities among many as illustrated in Scheme 1, we have taken up a study on the structural aspects of bisphenols by attaching an imidazole ring to it. It is also anticipated that such new imidazole containing bisphenols would bind to different anions depending on the availability of binding sites and the nature of the anion providing directional characteristics to self-assemblies. The number of such possible ways of interactions would increase when a bisphenol group is anchored to the imidazole part.

Received: December 30, 2011

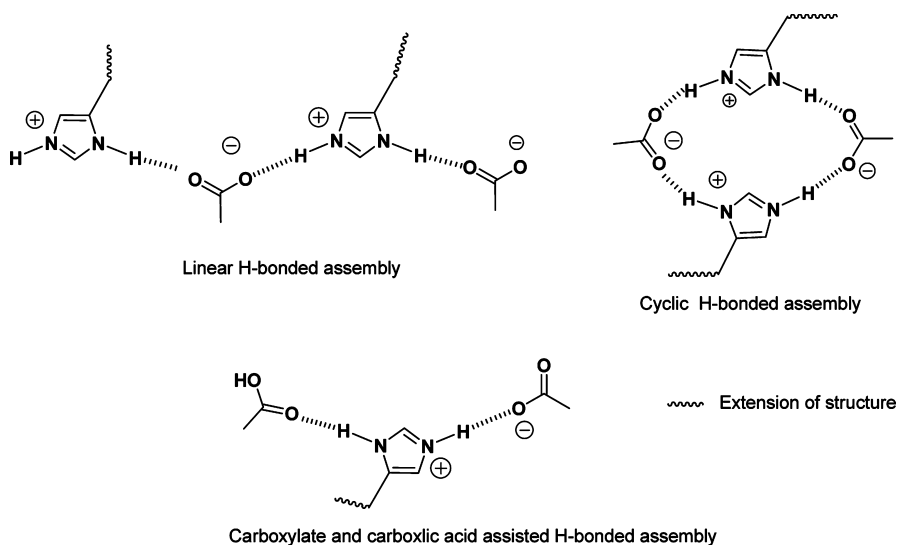
Revised: January 30, 2012

Published: February 6, 2012

Scheme 1. A Representative Case Showing Some Possible Ways through Which an Imidazolium Salt Bearing Bisphenol May Self-Assemble



Scheme 2. Some Possible Assemblies Arising from N-H...O<sup>-</sup> and N<sup>+</sup>-H...O<sup>-</sup> Interactions of Imidazolium Cation with Carboxylate/Carboxylic Acid Functionality



Thus, imidazolium cation bearing bisphenols would have diverse ways to interact with anions to form different types of supramolecular assemblies. Some of the ways of N-H...O and charge assisted N<sup>+</sup>-H...O<sup>-</sup> interactions of an imidazolium cation with a carboxylate anion or with a combination of carboxylate anion and neutral carboxylic acid are illustrated in Scheme 2.

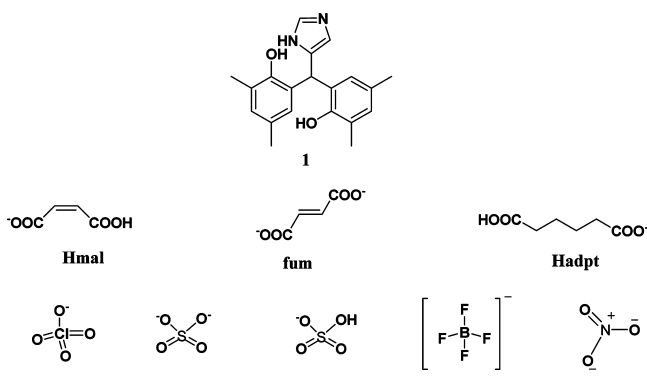
We have thus studied structural aspects of a series of salts of an imidazole containing bisphenol. The advantage of using salts rather than a neutral organic molecule for the designing of a supramolecular network is that the hydrogen bonding between ions is stronger than neutral organic molecules. Again, the role of the hydroxyl group would be interesting in guiding the interactions in the bisphenol molecule.

## RESULTS AND DISCUSSION

The imidazole containing bisphenol 2-((2-hydroxy-3,5-dimethylphenyl)(imidazol-4-yl)methyl)-4,6-dimethylphenol (**1**, abbreviated as Imbp) was prepared by a procedure reported for related bisphenols,<sup>16</sup> and it was crystallized as solvent free Imbp from dimethylsulfoxide and as methanol solvate Imbp·MeOH (**2**) from methanol. Here, we present the structural aspects of a series of imidazolium bisphenol salts that are derived from **1** on interaction with three different carboxylic acids, viz., maleic, fumaric, and adipic, and that bears inorganic anions, viz., perchlorate, sulfate, bisulphate, tetrafluoroborate, and nitrate anions (Scheme 3).

The bisphenol **1** (abbreviated as Imbp) crystallizes in monoclinic space group  $P2_1/n$  and has moderately strong hydrogen bonded structure in the form of self-assembly. There

**Scheme 3. Structure of the Imidazole Containing Bisphenol (1) and the Anions Used in This Study**

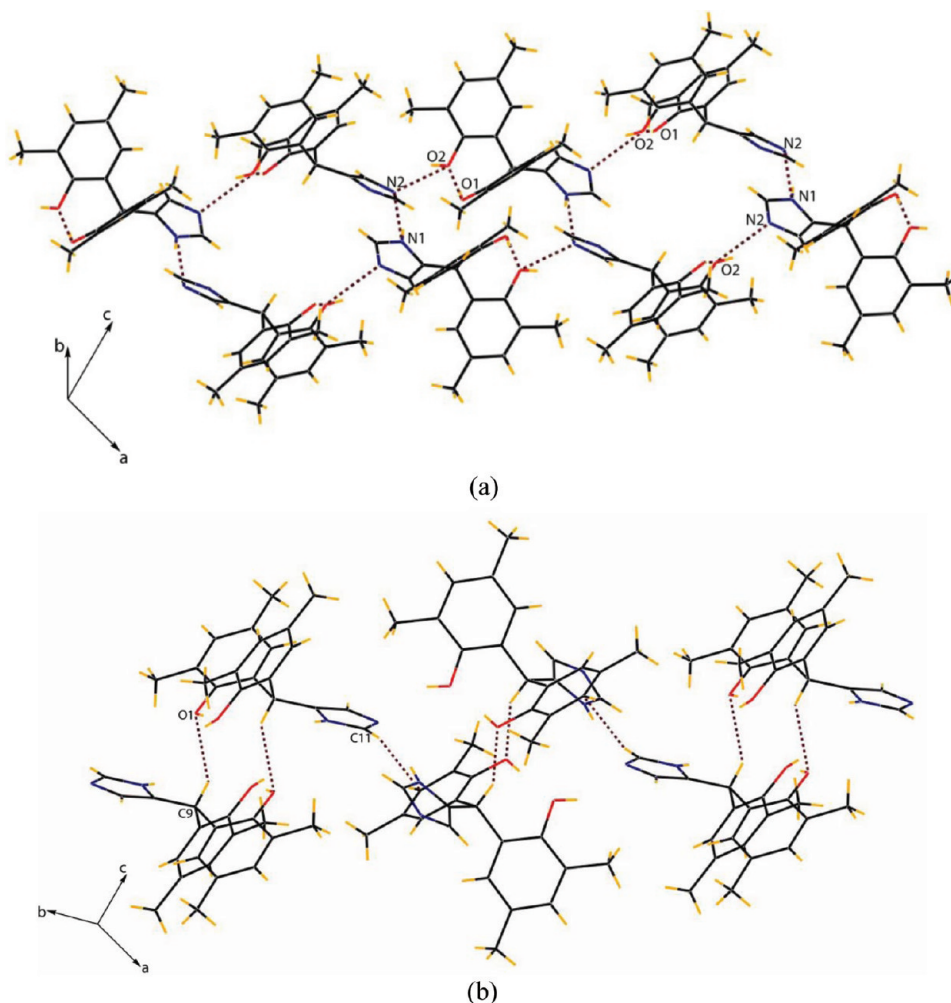


are two moderate H-bonds, viz.,  $\text{N}(1)-\text{H}(1\text{A})\cdots\text{N}(2)$  and  $\text{O}(2)-\text{H}(2)\cdots\text{N}(2)$  ( $\angle\text{D}-\text{H}\cdots\text{A}$ ;  $164^\circ$  and  $145^\circ$  and  $d_{\text{D}\cdots\text{A}}$  2.991(3), 2.816(3) Å respectively). The two hydroxy groups of each bisphenol molecule form strong intramolecular H-bonds with  $\angle\text{D}-\text{H}\cdots\text{A}$  as  $174^\circ$ ;  $d_{\text{D}\cdots\text{A}}$  2.720(3) Å. The combination of these H-bonds leads to the formation of two different types of cyclic H-bonding motifs as shown in Figure 1a. Apart from these H-bonds, there are some other interactions such as  $\text{C}-\text{H}\cdots\text{O}$  and  $\text{C}-\text{H}\cdots\pi$  interactions which also contribute to the

stability of the system. A few prominent interactions are shown in Figure 1b and bond parameters are listed in Table 1.

The methanol solvate of **1** Imbp·MeOH (**2**) crystallizes in triclinic space group  $P\bar{1}$  and its asymmetric unit contains a methanol molecule along with the Imbp molecule. Each methanol molecule in this solvate bridges two host molecules through  $\text{O}(2)-\text{H}(2)\cdots\text{O}(3)$  ( $d_{\text{D}\cdots\text{A}}$  2.664 Å;  $\angle\text{D}-\text{H}\cdots\text{A}$ ,  $155^\circ$ ) and  $\text{O}(3)-\text{H}(3\text{A})\cdots\text{N}(1)$  ( $d_{\text{D}\cdots\text{A}}$  2.748 Å;  $\angle\text{D}-\text{H}\cdots\text{A}$ ,  $177^\circ$ ) interactions. Such bridges lead to the formation of an infinite chainlike structure as illustrated in Figure 2. The NH group of the imidazole ring are involved in bifurcated hydrogen bonds with two hydroxy groups present in another neighboring bisphenol molecule via  $\text{N}-\text{H}\cdots\text{O}$  interactions ( $\text{N}(2)-\text{H}(2\text{A})\cdots\text{O}(1)$  ( $d_{\text{D}\cdots\text{A}}$  3.123 Å;  $\angle\text{D}-\text{H}\cdots\text{A}$ ,  $126^\circ$ ) and  $\text{N}(2)-\text{H}(2\text{A})\cdots\text{O}(2)$  ( $d_{\text{D}\cdots\text{A}}$  3.071 Å;  $\angle\text{D}-\text{H}\cdots\text{A}$ ,  $144^\circ$ )). Moreover, one of the hydroxy groups of the bisphenol molecule also are involved in bifurcated hydrogen bonding with the NH group and OH group of the solvent molecule through  $\text{N}-\text{H}\cdots\text{O}$  and  $\text{O}-\text{H}\cdots\text{O}$  interactions (Figure 2). Over and above these, the imidazole rings are placed parallel in the lattice with a plane-to-plane separation of 3.302 Å, and this distance of separation suggests  $\pi-\pi$  interaction among the imidazole rings.

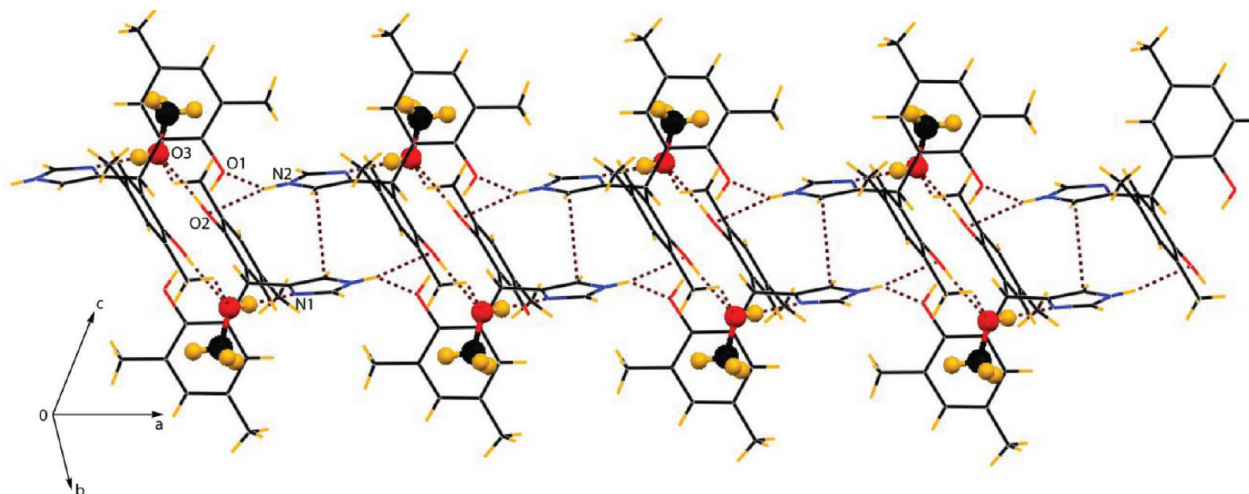
When the bisphenol **1** is treated with maleic acid ( $\text{H}_2\text{mal}$ ) it forms hydrated salt, namely, HImbp·Hmal· $\text{H}_2\text{O}$  (**3**). The salt **3** crystallizes in a monoclinic space group  $P2_1/c$ . The crystallo-



**Figure 1.** (a) Different types of cyclic H-bonding motifs in **1**. (b) Selected  $\text{C}-\text{H}\cdots\text{O}$  and  $\text{C}-\text{H}\cdots\pi$  interactions in **1**.

Table 1. Selected H-Bond Parameters of 1–5

compd. nos.	D–H...A	$d_{D-H}$ (Å)	$d_{H...A}$ (Å)	$d_{D...A}$ (Å)	$\angle D-H...A$ (°)
1	O(1)–H(1) ...O(2)	0.82	1.90	2.720(3)	174
	N(1)–H(1A) ...N(2) $[-1/2 - x, 1/2 + y, 1/2 - z]$	0.85(3)	2.17(3)	2.991(3)	164(3)
	O(2)–H(2) ...N(2) $[1/2 + x, 1/2 - y, 1/2 + z]$	0.82	2.11	2.816(3)	145
	C(9)–H(9) ...O(1)	0.98	2.48	2.905(3)	106
2	O(1)–H(1) ...O(2)	0.82	2.32	3.1352(18)	174
	O(2)–H(2) ...O(3) $[1 - x, 1 - y, -z]$	0.82	1.90	2.664(2)	155
	N(2)–H(2A) ...O(1) $[-1 + x, y, z]$	0.86	2.53	3.123(2)	126
	N(2)–H(2A) ...O(2) $[-x, 1 - y, -z]$	0.86	2.33	3.071(2)	144
	O(3)–H(3A) ...N(1)	0.82	1.93	2.748(2)	177
3	O(1)–H(1) ...O(7) $[x, 3/2 - y, -1/2 + z]$	0.89(3)	1.78(3)	2.669(2)	172(3)
	N(1)–H(1A) ...O(3) $[-x, 1 - y, -z]$	0.86	1.91	2.750(2)	166
	O(2)–H(2) ...O(1)	0.82	1.98	2.789(2)	167
	N(2)–H(2A) ...O(4) $[x, 3/2 - y, 1/2 + z]$	0.86	1.95	2.772(2)	158
	O(5)–H(5A) ...O(3)	0.82	1.61	2.425(2)	170
	O(7)–H(7E) ...O(5) $[-x, 1/2 + y, 1/2 - z]$	0.86(3)	2.07(3)	2.893(2)	160(3)
4	O(1)–H(1) ...O(3) $[1 - x, 1 - y, 1 - z]$	0.82	1.95	2.6950(17)	150
	N(1)–H(1A) ...O(4) $[-x, 1 - y, 1 - z]$	0.96(3)	1.75(3)	2.6712(18)	159(2)
	O(2)–H(2) ...O(1)	0.82	1.98	2.7953(18)	173
	N(2)–H(2A) ...O(3) $[-x, -y, 1 - z]$	0.90(3)	1.78(3)	2.6721(17)	169(2)
	O(5)–H(5A) ...O(4) $[1 + x, 1/2 - y, 1/2 + z]$	0.82	1.83	2.651(2)	175

Figure 2. Different types of hydrogen bonding and  $\pi$ – $\pi$  interactions in Imbp·MeOH (2).

graphic asymmetric unit consists of the HImbp cation, a maleate anion, and a water molecule of crystallization. Strong intramolecular H-bonding (O–H...O) is observed within the maleate ion. The maleate anion generally forms an intramolecular hydrogen bonded structure<sup>17</sup> and such anions participate in hydrogen bond formation with host molecules. In this case also this is not an exception but the water of interest in the structure is the unconventionality obtained in holding the anions by simultaneous hydrogen bonds with the water molecule acting as a bridge on one side and a direct hydrogen bond to the host cation (Figure 3a). Moreover, the two hydroxy groups of the host cation (HImbp) also are involved in intramolecular O(2)–H(2)...O(1) ( $d_{D...A}$  2.789 Å;  $\angle D-H...A$ , 167°) hydrogen bonding. The water molecule is coordinated to one hydroxy group of the host molecule and

two Hmal anions through O–H...O interactions and the Hmal anion forms water bridged zigzag polymeric chain. The Hmal anion interacts with the bisphenol through charge-assisted N–H (imidazole)...O<sup>–</sup> interactions (Figure 3).

It is shown that the maleic acid on reaction with **1** forms salt with mono-deprotonated acid, whereas its trans counterpart, namely, fumaric acid, formed a di-deprotonated salt with the cation of the bisphenol **1**. For charge balance, two molecules of imidazolium bisphenol cation accept one fumarate anion to give HImbp·0.5 fum (**4**). The  $pK_{a2}$  of these two acids is 6.62 for maleic acid and 4.44 for fumaric acid; the difference is due to geometry of the acids. The former acid adopts a strong intramolecular hydrogen bonded structure upon first deprotonation. The salt **4** crystallizes in triclinic space group  $P\bar{1}$  and the crystallographic asymmetric unit contains one host cation,



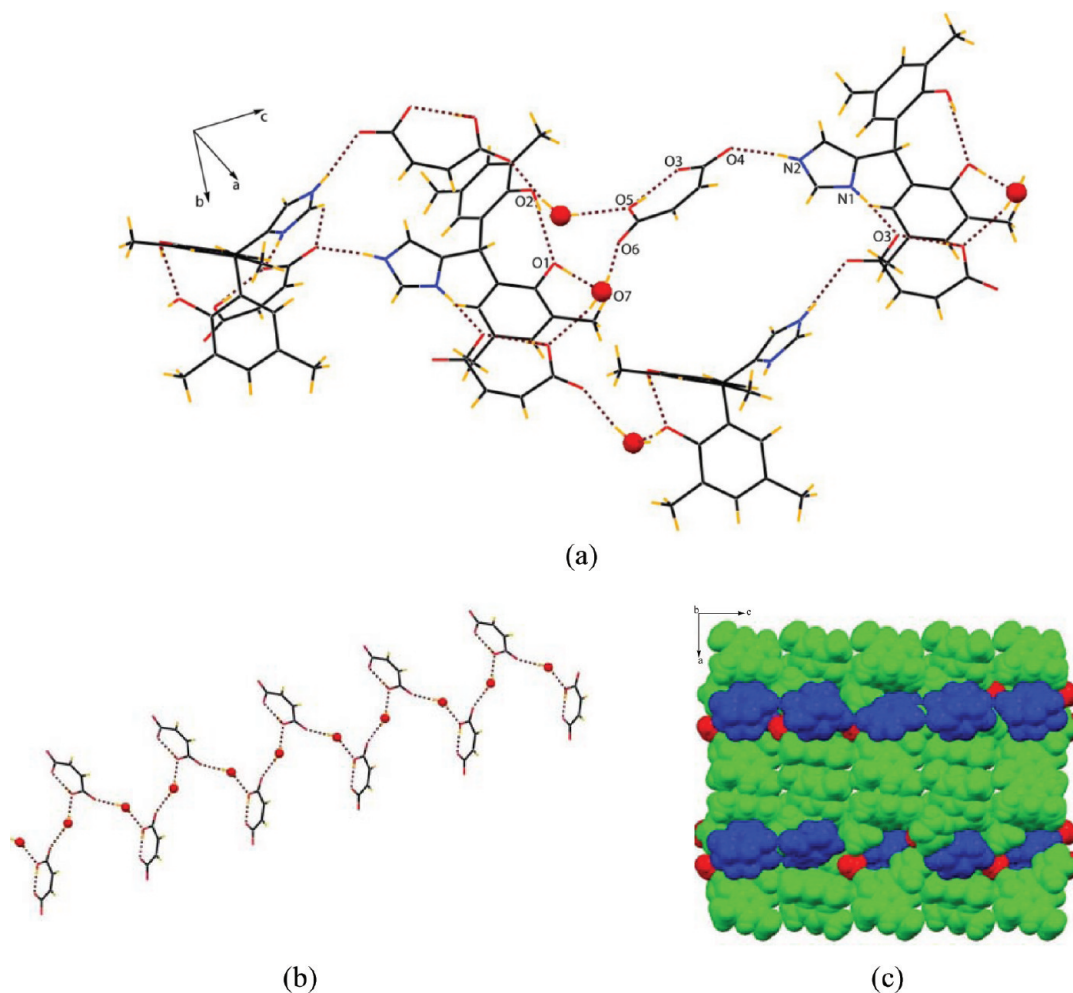


**Figure 3.** (a) The C–H...O, N–H...O, and O–H...O interactions in **3**. (b) Formation of zigzag 1D chain of maleate monoanion and water through H-bonding in **3**. (c) Spacefill model of **3**, green = host cation, blue = maleate anion, red = water molecule.

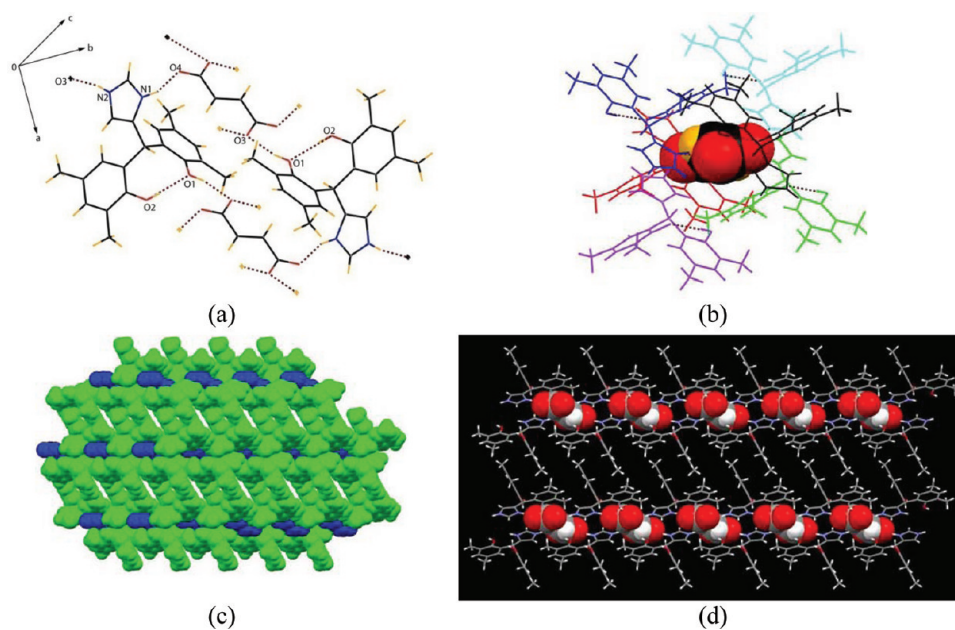


**Figure 4.** (a) Formation of the assembly of host with two fumerate ions in **4**. (b) Encapsulation of fumerate ions in the hexameric assembly of the host cations in **4**. (c) Spacefill model of the complex (blue is fumerate anion and green is host cation). (d) Packing diagram showing the layered structure when viewed along the crystallographic *a*-axis.

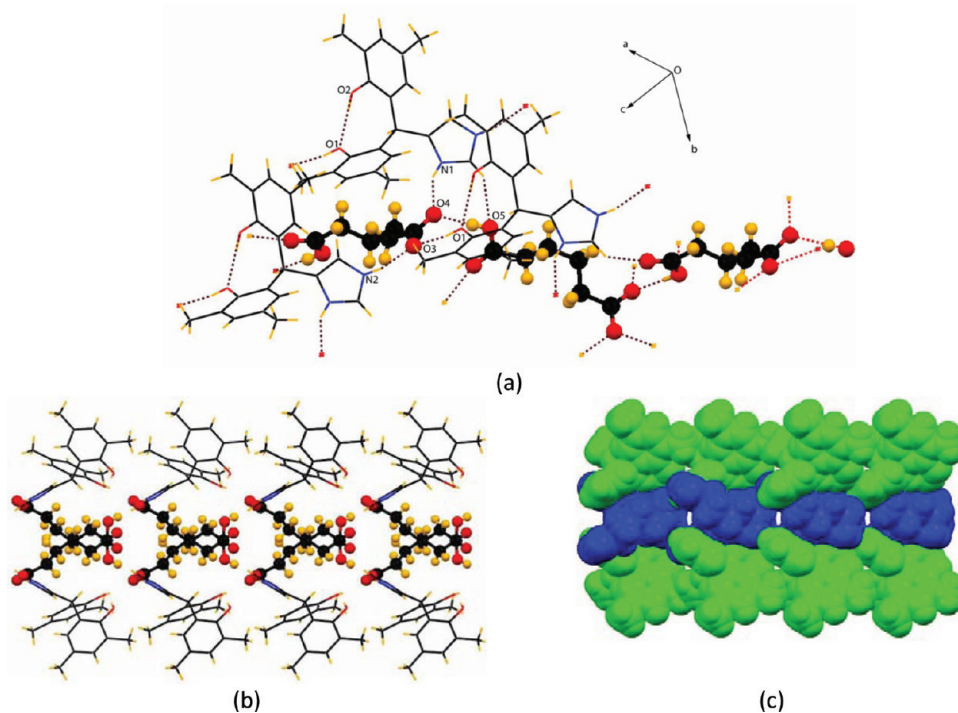


**Figure 5.** (a) One-dimensional zigzag H-bonding chain of adipate ion showing all the H-bonding interactions in HImbp-Hadpt (**5**). (b) Packing of the molecules in **5** when viewed along the crystallographic *c*-axis. (c) Spacefill model of the complex **5** (blue for Hadpt and green for HImbp).

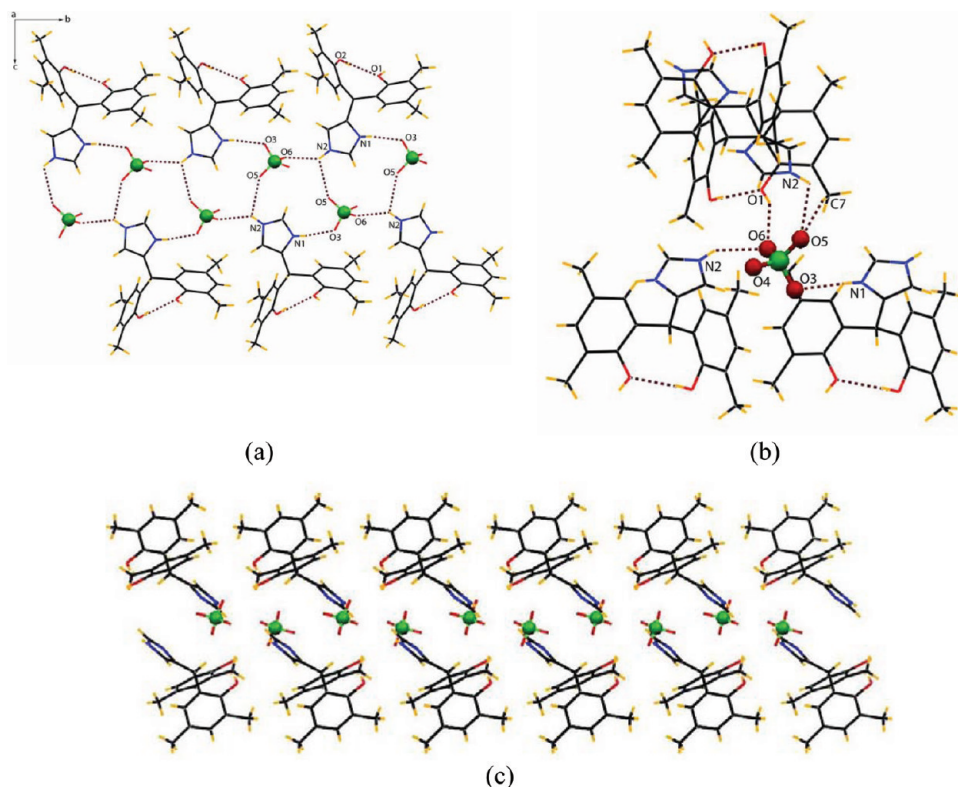


**Figure 6.** (a)  $N^+–H\cdots O^-$ ,  $N–H\cdots O$ , and  $O–H\cdots O$  interactions in HImbp- $ClO_4$  (**6**) to form a H-bonded ladder. (b) Interaction of the perchlorate anion through  $N^+–H\cdots O$ ,  $N–H\cdots O$  and  $O–H\cdots O$  and  $C–H\cdots O$  interaction. (c) Formation of a layered structure which incorporates perchlorate anions.

HImbp, and the half of the fumarate anion. The host molecules form dimers with two fumarate ions through  $N–H$  (imidazole) $\cdots O^-$  and  $O–H\cdots O$  interactions (Figure 4a). The intramolecular  $O2–H\cdots O1$  interaction in the host molecule is

also observed as in the earlier case. Each fumarate ion interacts with six host molecules through  $N–H$  (imidazole) $\cdots O^-$  and  $O–H\cdots O$  interactions, resulting in the encapsulation of the anion in the hexameric cavity formed by the host cation (Figure

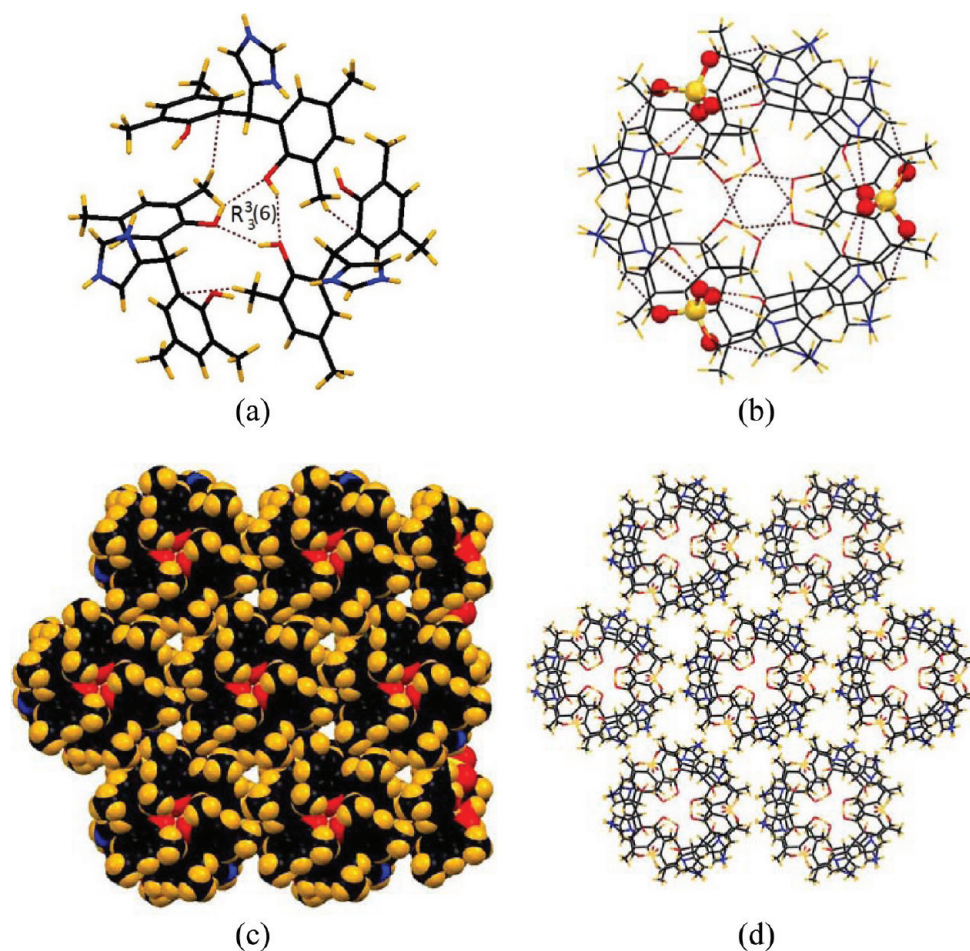


**Figure 7.** (a) Formation of trimeric assembly of HIMbp through  $R_3^3(6)$  type cyclic H-bonding in HIMbp·0.5SO<sub>4</sub><sup>2-</sup> (7). (b) Interaction of two trimeric assemblies through sulfate anion leading to a bowl like structure. (c) Packing of the crystal in spacefill model. (d) Packing of the molecules in the crystal lattice viewed along the crystallographic *c*-axis.

4b). Here N–H (imidazole) acts as H-bond donor and the oxygen (carboxylate) acts as a H-bond acceptor and finally the salt forms a layered structure (Figure 4d). The salt of imidazole and fumaric acid have a layered structure.<sup>15</sup> In our system, the complexity provided by the weak interactions of the phenolic units forces the system to self-assemble to bind to the fumarate anion.

The bisphenol **1** also forms salt of mono-deprotonated adipic acid (Hadpt) HIMbp·Hadpt (**5**). The salt formation by the mono-deprotonation of this acid is rational as it has a  $pK_{a1}$  value of 4.42, which is comparable to the  $pK_{a2}$  value of the fumaric acid. The salt **5** crystallizes in monoclinic space group  $P2_1/c$  and the crystallographic asymmetric unit contains the host cation and mono-deprotonated adipate ion. The adipate monoanions form a 1D zigzag chain through O–H···O interactions between the hydroxyl group of the carboxylic acid (H-bond donor) and the O<sup>-</sup> carboxylate (H-bond acceptor) (Figure 5a). Each oxygen atom of the carboxylate group of the adipate ion is involved in a bifurcated H-bond (O–H···O and N–H···O interactions). The hydrogen bond parameters are listed in Table 1. The adipate anion adopts a bent conformation different from the parent adipic acid structure in the unsolvated form.<sup>18</sup> The bent structure of adipic acid is also observed in the cocrystal of adipic acid with cytosine.<sup>19</sup> Finally the salt forms a sheetlike structure in which the Hadpt anions are incorporated between the two layers

formed by the host cations as shown in Figure 5b,c. The formation of salt in the cases of **3–5** were also confirmed by infrared spectroscopy in the solid state. The carbonyl stretching frequency of the carboxylate groups are shifted toward lower frequency compared to the free carboxylic acid upon salt formation. In the case of HIMbp·Hadpt and HIMbp·Hmal·H<sub>2</sub>O, it is seen that two different C=O stretching frequencies appear around 1536–1574 cm<sup>-1</sup> and 1711–1717 cm<sup>-1</sup> for carboxylate and carboxylic acid.

The perchlorate salt of **1**, HIMbp·ClO<sub>4</sub> (**6**) crystallizes in a monoclinic space group  $P2_1/c$ , and its asymmetric unit contains one protonated host molecule and a perchlorate anion. Both the N–H and the N<sup>+</sup>–H group of the imidazole ring act as a H-bond donor and engage in hydrogen bonding with the perchlorate ion forming a ladder like H-bonded network when viewed along the *a*-axis. These types of supramolecular features were found in the crystal structure of theophylline-perchlorate salt.<sup>20</sup> As in the earlier cases, the hydroxy groups of the host cation are involved in intramolecular H-bonds (Figure 6a). Over and above these, one of the hydroxy groups participating in the intramolecular hydrogen bond has a hydrogen atom free, which acts as H-bond donor to the oxygen atom of the perchlorate anion. Each perchlorate ion interacts with four guest cations through N–H···O, O–H···O, and C–H···O interactions (Figure 6b). Finally, the salt forms two discrete layered sheets in two different crystallographic



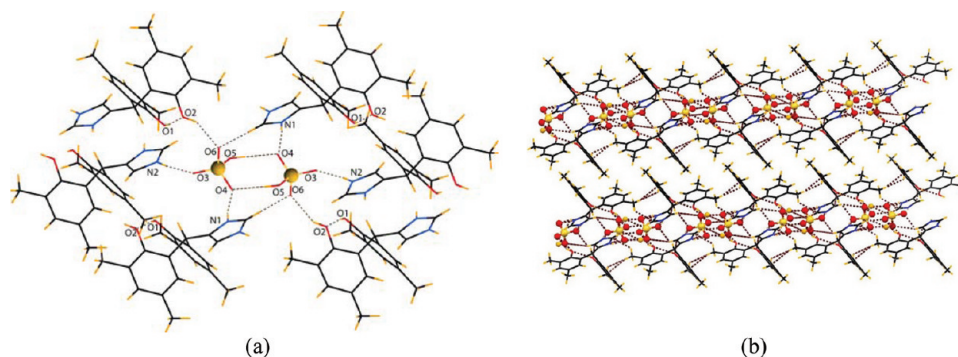


**Figure 8.** (a) Formation of  $R_2^2(6)$  types of cyclic H-bonding by the bisulphate anion. HImbp- $\text{HSO}_4$ . (b) Two discrete parallel sheets in HImbp- $\text{HSO}_4$ , viewed along the crystallographic  $a$ -axis.

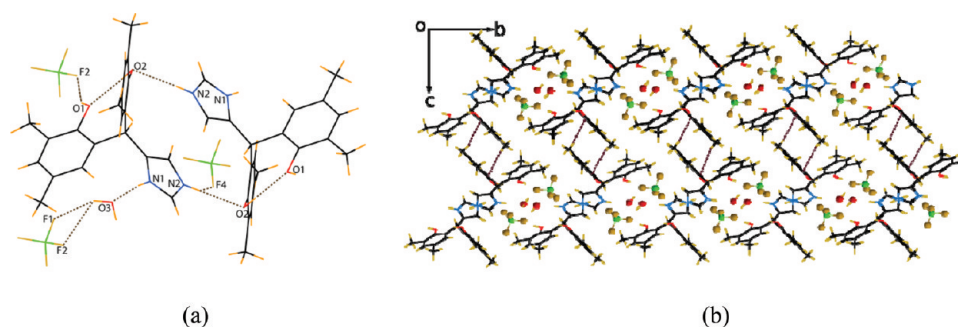


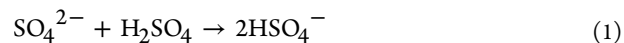
**Figure 9.** (a) Dimer of host cations through N-H $\cdots$ O interactions in HImbp- $\text{BF}_4$ . (b) The C-H $\cdots$  $\pi$  interactions between the sheetlike structures of HImbp- $\text{BF}_4$ .

directions and each sheet is stabilized by perchlorate anions (Figure 6c).

The sulfate salt of **1**, HImbp- $0.5\text{SO}_4^{2-}$  (**7**), is in a 1:0.5 ratio of cation and anion; it crystallizes in the space group  $R3_2$  and the crystallographic asymmetric unit contains one HImbp molecule and the half of the sulfate ion. The two cations are mainly held together by electrostatic interaction and H-bonding. The O3 of the sulfate anion is involved in bifurcated H-bonding with the host cation through N-H $\cdots$ O and O-H $\cdots$ O, and the O4 of the sulfate anion are involved in trifurcated H-bonding with the host cation through N-H $\cdots$ O and C-H $\cdots$ O interaction. One of the hydroxyl groups of the host molecule is involved in intermolecular H-bonding (both as donor and acceptor) with the same hydroxyl group of another two similar host molecules forming a trimeric assembly through  $R_3^3(6)$  types of cyclic hydrogen bonding (Figure 7a). The other hydroxy groups and the imidazole rings of this trimeric assembly projects upward and gives rise to a cyclic type of structure that has a resemblance to calix arene. Two such trimeric assemblies are further connected to the O3 of three sulfate anions through N-H $\cdots$ O and O-H $\cdots$ O interactions. These interactions lead to formation of circular assemblies when viewed along the  $c$ -axis (Figure 7b). These circular assemblies are connected to each other by O4 of sulfate through N2-H $\cdots$ O4 interactions completing the three-dimensional structure. Three such assemblies are found to be in contact with each other in the crystal lattice (Figure 7c,d).

A bisulphate salt of bisphenol **1** was formed serendipitously. When magnesium sulfate hexahydrate was treated with bisphenol **1** in aqueous methanol, it led to formation of

HImbp- $\text{HSO}_4$  (**8**). The formation of the bisulphate salt is attributed to hydrolytic



disproportionation of magnesium sulfate in methanol as shown in eq 1. The 1:1 salt **8** crystallizes in the  $P\bar{1}$  space group and the crystallographic asymmetric unit contains one HImbp cation and bisulphate anion. The two molecules are mainly held together by electrostatic and H-bonding interactions. The  $\text{HSO}_4$  anions form a dimeric structure through  $R_2^2(6)$  types of cyclic H-bonds, and these dimers are held in the assembly of the protonated host molecules of Imbp through O-H $\cdots$ O and N-H $\cdots$ O interactions involving the hydroxyl and the N-H groups of Imbp (Figure 8a). The N $^+$ -H of the protonated imidazole also serves as a H-bond donor to the guest anion. There are no strong intermolecular interactions among the host cations, but the two hydroxy groups of the host cation are involved in intramolecular H-bond interactions. When we viewed the packing pattern from the crystallographic  $a$ -axis, it is seen that the molecules form two discrete sheets and each sheet incorporates the  $\text{HSO}_4$  anion. Hydrogen sulfate salts have found applications in various devices such as  $\text{H}_2$  and  $\text{H}_2\text{O}$  sensors, fuel and stream cells, and high-energy-density batteries.<sup>21</sup> Braga et al. have reported the crystal structure of the stabilized hydrogen sulfate adducts of crown ethers.<sup>22</sup> Hydrogen sulfate salts are of interest in supramolecular aspects and crystal engineering because of its analogy to biologically relevant biphosphate anion and the presence of H-bonding between the ions for self-association.<sup>23</sup> In a recent study, the stabilization of the bisulphate anion along with the sulfate anion by 3,5-diphenylpyrazole has been reported.<sup>24</sup> In our earlier studies, the stabilization of methyl and ethyl sulfate salts by various bisphenol hosts has been reported.<sup>13,25</sup>



Table 2. Selected H-Bond Parameters of 6–10

compd. nos.	D–H...A	$d_{D-H}(\text{\AA})$	$d_{H...A}(\text{\AA})$	$d_{D...A}(\text{\AA})$	$\angle D-H...A(^{\circ})$
6	O(1)–H(1) ...O(6)	0.74(6)	2.07(6)	2.719(7)	146(5)
	N(1)–H(1A) ...O(3) [x, 3/2 – y, –1/2 + z]	0.79(6)	2.14(6)	2.895(6)	161(5)
	O(2)–H(2) ...O(1)	0.82	2.01	2.817(5)	170
	N(2)–H(2A) ...O(6) [x, 1/2 – y, –1/2 + z]	0.93(7)	2.23(7)	2.988(6)	138(6)
7	O(1)–H(1) ...O(1) [–y, x – y, z]	0.82	2.15	2.864(8)	146
	N(1)–H(1A) ...O(3) [–y, x – y, z]	0.86	1.91	2.759(8)	171
	O(2)–H(2) ...O(3)	0.82	2.15	2.826(7)	140
	N(2)–H(2A) ...O(4) [1 – x, 1 – x + y, –z]	0.86	1.86	2.719(8)	176
8	O(1)–H(1) ...O(2)	0.82	1.99	2.800(2)	169
	N(1)–H(1A) ...O(4) [x, –1 + y, 1 + z]	0.83(2)	2.07(2)	2.869(2)	162.1(18)
	O(2)–H(2) ...O(6) [–x, 1 – y, 1 – z]	0.82	2.07	2.818(2)	151
	N(2)–H(2A) ...O(3) [1 + x, –1 + y, 1 + z]	0.86(3)	2.05(2)	2.888(2)	165.6(18)
9	O(5)–H(5A) ...O(4) [1 – x, 1 – y, –z]	0.82	1.93	2.738(2)	169
	O(1)–H(1) ...F(2) [1 + x, 1 + y, z]	0.82	2.11	2.832(3)	146
	N(1)–H(1A) ...O(3) [1 – x, 1 – y, 1 – z]	0.86(4)	1.89(4)	2.729(5)	166(3)
	O(2)–H(2) ...O(1)	0.82	2.05	2.853(3)	166
10	N(2)–H(2A) ...F(4)	0.91(3)	2.21(3)	2.886(5)	131(3)
	N(2)–H(2A) ...O(2) [1 – x, 1 – y, 1 – z]	0.91(3)	2.18(4)	2.939(3)	140(3)
	O(3)–H(3N) ...F(1) [1 – x, –y, 1 – z]	0.82(9)	2.32(10)	2.997(5)	140(8)
	O(1)–H(1) ...O(3)	0.85(13)	1.93(12)	2.762(7)	167(12)
	O(1)–H(1) ...O(5)	0.85(13)	2.36(14)	2.999(8)	133(9)
	N(1)–H(1A) ...O(5) [–1 + x, y, z]	0.86	1.98	2.765(6)	152
O(2)–H(2) ... O(1)	0.82	1.98	2.791(6)	170	
N(2)–H(2A) ...O(3) [x, y, 1 + z]	1.00(7)	1.84(8)	2.803(6)	162(7)	
N(2)–H(2A) ...O(4) [x, y, 1 + z]	1.00(7)	2.46(8)	3.249(8)	135(8)	

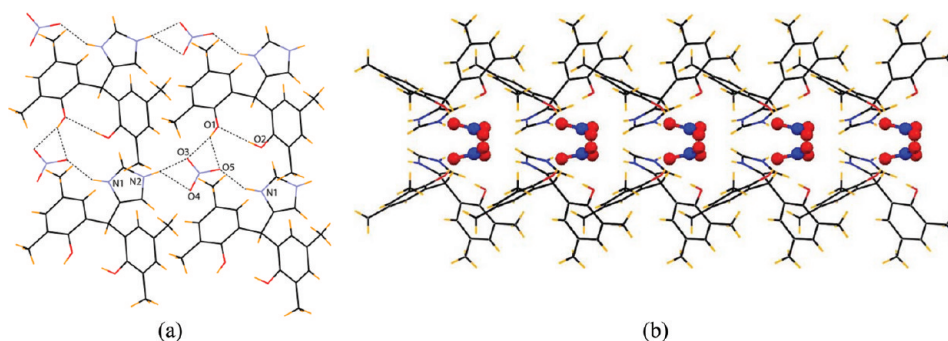


**Figure 10.** (a)  $N^+-H...O^-$ ,  $N-H...O$ , and  $O-H...O$  interactions in  $HImbp\cdot NO_3$  to form the sheetlike structures. (b) Packing of the molecules in  $HImbp\cdot NO_3$  viewed along the crystallographic  $c$ -axis.

The reaction of sodium tetrafluoroborate in wet methanol forms 1:1 salt of **1**,  $HImbp\cdot BF_4\cdot H_2O$  (**9**) which crystallizes in a triclinic space group  $P\bar{1}$ . The crystallographic asymmetric unit contains the host cation  $HImbp$ , tetrafluoroborate anion, and water molecule of crystallization. Formation of such salts from sodium tetrafluoroborate may be considered as unique as it is formed through a hydrolytic reaction between sodium tetrafluoroborate with water leading to the corresponding acid tetrafluoroboric acid and in such process the counter base has to be sodium hydroxide. We had an earlier observation on stabilization of tetrafluoroborate anion in a quinoline based receptor, in which we obtained protonated quinoline derivative by similar hydrolytic reaction of sodium tetrafluoroborate in wet DMF.<sup>26</sup> In the salt **9**, the water of crystallization molecule acts as a donor toward the tetrafluoroborate anion and acceptor toward  $N-H$  of the imidazole ring. The protonated  $N^+-H$  of the imidazole ring is involved in bifurcated H-bonding with one of the hydroxyl groups of the host cation and to the tetrafluoroborate anion. The host cation forms a dimer through

$N(2)-H(2A)...O(2)$  hydrogen bonding interactions (Figure 9a). These dimers are connected to each other via two water molecules and two tetrafluoroborate anions through  $N-H...O$ ,  $O-H...F$ , and  $N-H...F$  interactions (Table 2). Such interactions lead to the formation of sheetlike structures parallel to the  $bc$ -plane (Figure 9b). These sheetlike structures intercalate tetrafluoroborate anions and are held together by  $C-H...π$  interactions as shown in Figure 9b.

Finally, we have prepared the salt of **1** with a planar anion, namely, nitrate anion. The nitrate salt  $HImbp\cdot NO_3$  (**10**) is a 1:1 electrolyte and crystallizes in a monoclinic space group  $P2_1/c$ . The crystallographic asymmetric unit of **10** contains one host cation and a nitrate anion. Both the  $N^+-H$  and  $N-H$  bonds of the imidazole act as H-bond donor toward the nitrate anion (Figure 10a). In this case also, two hydroxy groups of the host cation are involved in intramolecular H-bonding. The hydrogen atom not participating in the cyclic structure of intramolecular hydrogen bond acts as H-bond donor to the nitrate anion. This assembly forms a sheet parallel to the  $ac$ -plane which

incorporates the nitrate anions as shown in the Figure 10b. The parameters of the H-bond interactions in the assembly of 10 are listed in Table 2.

The powder X-ray diffraction (PXRD) of the samples was recorded (please refer to Supporting Information) to see if there are any other types of structural units in the salts. We have found a good agreement on experimental and simulated PXRD data for all the salts, and it suggests the uniformity of the structural features of the bulk materials. The formation of salts in case of 6–10 is also confirmed by  $^1\text{H}$ NMR spectra, as the N–H protons on the imidazole ring shifted to a higher  $\delta$ -value on interaction with anions (please refer to Supporting Information). We have studied the preferential crystallization process of these salts by adding the salts to another acid solution. We have observed that weak perchlorate anion or nitrate anion can be successfully replaced by sulfate anion from their respective salt. However, the reverse process, namely, the sulfate salt, does not lead to formation of perchlorate or nitrate salt on treatment with perchloric acid and nitric acid, respectively. Because of the lack of distinguishable and characteristic absorption maxima in the UV region of the carboxylate salts that we have presented here, we have not carried out the competitive binding of carboxylate anions.

The DSC of the crystalline solids of 3–5 show a flat baseline with sharp peaks, which is also consistent of the high purity of the bulk materials. The HImbp-Hmal-H<sub>2</sub>O, HImbp-fum, and HImbp-Hadpt show endothermic peaks at 274, 247, and 216 °C, whereas the melting point of Imbp is 240 °C. From the TG analysis of HImbp-Hmal-H<sub>2</sub>O (3), it is seen that the water of crystallization is lost at around 134 °C from the hydrated form of the salt, which indicates that the water molecule is strongly bound in the assembly. Whereas in the case HImbp-BF<sub>4</sub>-H<sub>2</sub>O (9), the water of crystallization is lost at around 85 °C, in this case water molecules are attached to two dimeric assemblies of the cations and are relatively weakly bound compared to water molecules in 3.

## CONCLUSIONS

A large number of structural variations by directional hydrogen bonds in anion assisted assemblies of an imidazole containing bisphenol are shown. The structural versatilities in terms of the deprotonation process, structure, and charge on anions as well as compositions of guest host assemblies are illustrated. Among the two isomeric cis and trans dicarboxylic acids, maleic acid (cis) led to the monodeprotonated salt, whereas fumeric acid (trans) led to the dideprotonated salt; in the former case a water-assisted sheetlike layered structure is observed. In the latter case anion encapsulated assembly is formed through assembling of cations. Among the tetrahedral anions sulfate led to trimeric subassemblies of the cationic bisphenol part which is held together by sulfate ions forming assemblies with circular shapes. The intramolecular H-bonding between the phenolic hydroxy groups of the bisphenol molecules is observed in all the cases except in the case of the sulfate salt (7). It is attributed to large electrostatic interactions offered by the sulfate dianion. The formation of the tetrafluoroborate salt of 1 from sodium tetrafluoroborate in methanol is a very rare phenomenon. Finally, bisulphate anion is trapped from the acidolysis of magnesium sulfate and sulphuric acid in methanol, and stabilization of bisulphate anion by bisphenol guest from this reaction is unprecedented to best of our knowledge.

## EXPERIMENTAL SECTION

**Synthesis of 2-((2-Hydroxy-3,5-dimethylphenyl)(imidazol-4-yl)methyl)-4,6-dimethylphenol (1).** 4(S)-Imidazole carboxaldehyde (0.48 g, 5 mmol) and 2,4-dimethylphenol (1.22 g, 10 mmol) were dissolved in acetic acid (20 mL) and the solution was stirred for half an hour in an ice bath. A mixture of concentrated sulphuric acid and glacial acetic acid in a 1:2 ratio (10 mL, v/v) was added dropwise to the reaction mixture. After half an hour of stirring, the mixture was kept in a deep freeze for one week. After one week, ice cold water (10 mL) was added to the reaction mixture; a white precipitate appeared. The reaction mixture was filtered and the precipitate was washed with aqueous sodium bicarbonate solution (20%, 25 mL). The product was then dried in air. Yield, 87%.  $^1\text{H}$ NMR (400 MHz, DMSO-*d*<sub>6</sub>): 2.09 (s, 6H), 2.11 (s, 6H), 5.74 (s, 1H), 6.71 (s, 2H), 6.85 (s, 2H), 7.73 (s, 1H). ESI mass: [M + 1]: 323.0767. IR (cm<sup>-1</sup>): 3840 (w), 3439 (s), 3148 (m), 2912(w), 1615 (s), 1550 (s), 1486 (s), 1440 (m), 1325 (m), 1226 (s), 1185 (m), 1094 (w), 1012 (w), 935 (w), 856 (w), 751 (w), 658 (w). 2-((2-hydroxy-3,5-dimethylphenyl)(imidazol-4-yl)methyl)-4,6-dimethylphenol was crystallized in the solvent free form 1, from dimethylsulfoxide and solvated form as Imbp-MeOH (2) from methanol.

**HImbp-Hmal-H<sub>2</sub>O (3).** Equimolar amounts (0.5 mmol) of Imbp (0.161 g) and maleic acid (0.058 g) were dissolved in methanol (10 mL) and kept for crystallization. After one week, colorless crystals appeared. Yield, 96%. IR (cm<sup>-1</sup>): 3461 (s), 3135 (m), 2920 (m), 1620 (s), 1578 (s), 1489 (s), 1443 (m), 1387 (m), 1363 (s), 1298 (w), 1212 (s), 1149 (w), 1089 (w), 993 (w), 863 (s), 788 (w), 751 (s), 661 (w), 625 (w), 568 (w).

**HImbp-0.5fum (4).** Imbp (0.322 g, 1 mmol) and fumeric acid (0.058 g, 0.5 mmol) were dissolved in methanol (15 mL) and kept for crystallization. After one week colorless crystals appeared. Yield, ~94%. IR (cm<sup>-1</sup>): 3324 (s), 3140 (m), 2916 (s), 2569 (m), 1538 (s), 1489 (s), 1443 (s), 1352 (m), 1325 (m), 1304 (m), 1289 (m), 1228 (s), 1166 (s), 1101 (m), 988 (s), 920 (w), 874 (w), 846 (m), 790 (m), 750 (m), 674 (s), 641 (w), 620 (w), 574 (w).

**HImbp-Hadpt (5).** Equimolar amounts (0.5 mmol) of Imbp (0.161 g) and adipic acid (0.146 g) were dissolved in methanol (10 mL) and allowed to stand for a week; colorless crystals were formed. Yield, 96%. IR (cm<sup>-1</sup>): 3439 (s), 3313 (s), 3159 (s), 2923 (s), 2862 (m), 2626 (w), 1711 (s), 1610 (s), 1536 (s), 1481 (s), 1443 (m), 1426 (m), 1327 (s), 1300 (m), 1262 (s), 1229 (s), 1166 (m), 1094 (w), 982 (w), 919 (w), 853 (m).

**HImbp-ClO<sub>4</sub> (6).** Equimolar amounts of Imbp (0.161 g, 0.5 mmol) and HClO<sub>4</sub> were dissolved in methanol (10 mL) and solution was left for crystallization. Colorless crystals were formed after one week. Yield, 93%. IR (cm<sup>-1</sup>): 3391 (s), 3159 (s), 3010 (m), 2917 (m), 1613 (s), 1487 (s), 1378 (w), 1337 (w), 1298(m), 1229(m), 1182 (m), 1142 (s), 1120 (s), 1087 (s), 1031(m), 984 (w), 929 (w), 866 (w), 806 (w), 789 (w), 624 (s).

**HImbp-0.5SO<sub>4</sub> (7).** Imbp (0.322 g, 1 mmol) and H<sub>2</sub>SO<sub>4</sub> in a 2:1 molar ratio were dissolved in methanol (15 mL) and kept for crystallization. Colorless crystals were formed after one week. Yield 96%. IR (cm<sup>-1</sup>): 3391 (s), 3136 (s), 2856 (s), 1617 (s), 1490 (s), 1377 (w), 1340 (w), 1191 (s), 1154 (s), 1093 (m), 1060 (s), 931 (w), 864 (s), 817 (m), 787 (w), 750 (w), 590 (s).

**HImbp-HSO<sub>4</sub> (8).** Imbp (0.322 g, 1 mmol) and magnesium sulfate heptahydrate (0.124 g, 0.5 mmol) were dissolved in methanol and then a few drops of sulphuric acid was added to it and the clear solution thus obtained was kept undisturbed. After 3 days pink colored crystals appeared. Yield, 91%. IR (cm<sup>-1</sup>): 3397 (s), 3131 (w), 3025 (w), 2918 (w), 1617 (s), 1483 (s), 1376 (w), 1340 (w), 1192 (w), 1154 (w), 1093 (m), 1060 (m), 931 (w), 864 (s), 589 (s), 493 (w).

**HImbp-BF<sub>4</sub>-H<sub>2</sub>O (9).** Equimolar amounts (0.5 mmol) of Imbp (0.161 g) and NaBF<sub>4</sub> (0.055 g) were dissolved in methanol (15 mL) and kept for crystallization. After one week, colorless crystals formed were filtered. Yield, 94%. IR (cm<sup>-1</sup>): 3344 (s), 3151 (m), 3016 (s), 2915 (m), 2851 (w), 1614 (m), 1551 (s), 1489 (s), 1439 (m), 1329 (w), 1303 (w), 1229 (s), 1185 (m), 1084 (w), 856 (w), 788 (w), 751 (w), 660 (w), 631 (w).

Table 3. Crystallographic Parameter of 1–10

compound no.	1	2	3	4	5
formulas	C <sub>20</sub> H <sub>22</sub> N <sub>2</sub> O <sub>2</sub>	C <sub>21</sub> H <sub>26</sub> N <sub>2</sub> O <sub>3</sub>	C <sub>24</sub> H <sub>28</sub> N <sub>2</sub> O <sub>7</sub>	C <sub>22</sub> H <sub>24</sub> N <sub>2</sub> O <sub>4</sub>	C <sub>26</sub> H <sub>32</sub> N <sub>2</sub> O <sub>6</sub>
CCDC no.	859874	859875	859878	859877	859876
mol wt	322.14	354.14	456.48	380.43	468.54
space group	<i>P</i> 2 <sub>1</sub> / <i>n</i>	<i>P</i> $\bar{1}$	<i>P</i> 2 <sub>1</sub> / <i>c</i>	<i>P</i> $\bar{1}$	<i>P</i> 2 <sub>1</sub> / <i>c</i>
<i>a</i> /Å	13.7298(6)	8.7555(8)	15.7164(10)	8.0009(3)	8.0566(5)
<i>b</i> /Å	9.1144(4)	10.3506(10)	9.2068(5)	9.2227(3)	33.229(2)
<i>c</i> /Å	14.9435(6)	11.3880(12)	16.0795(10)	13.6691(5)	9.1803(7)
$\alpha$ /°	90.00	79.478(7)	90.00	90.928(2)	90.00
$\beta$ /°	90.00	70.873(6)	90.744(4)	102.486(2)	101.130(5)
$\gamma$ /°	90.00	79.682(6)	90.00	103.478(2)	90.00
<i>V</i> / Å <sup>3</sup>	1747.40(13)	950.73(16)	2326.5(2)	955.31(6)	2411.5(3)
density/Mg m <sup>-3</sup>	1.225	1.238	1.303	1.323	1.291
abs coeff/mm <sup>-1</sup>	0.080	0.083	0.096	0.092	0.092
<i>F</i> (000)	688	380	968	404	1000
total no. of reflections	2910	3416	4484	3424	5997
reflections, <i>I</i> > 2σ( <i>I</i> )	2407	2790	2945	2943	3655
max $\theta$ /°	24.99	25.50	26.00	25.50	28.47
ranges ( <i>h</i> , <i>k</i> , <i>l</i> )	−15 ≤ <i>h</i> ≤ 15 −10 ≤ <i>k</i> ≤ 10 −16 ≤ <i>l</i> ≤ 16	−10 ≤ <i>h</i> ≤ 10 −12 ≤ <i>k</i> ≤ 12 −13 ≤ <i>l</i> ≤ 13	−18 ≤ <i>h</i> ≤ 19 −11 ≤ <i>k</i> ≤ 8 −19 ≤ <i>l</i> ≤ 18	−9 ≤ <i>h</i> ≤ 9 −11 ≤ <i>k</i> ≤ 11 −16 ≤ <i>l</i> ≤ 16	−9 ≤ <i>h</i> ≤ 9 −11 ≤ <i>k</i> ≤ 11 −16 ≤ <i>l</i> ≤ 16
complete to 2θ (%)	95.0	96.3	98.0	96.2	98.5
data/restraints/parameters	2910/0/227	3416/0/247	4484/0/316	3424/0/267	5997/0/314
GOF ( <i>F</i> <sup>2</sup> )	0.993	1.053	0.706	0.926	0.806
<i>R</i> indices [ <i>I</i> > 2σ( <i>I</i> )]	0.0577	0.0518	0.0505	0.0420	0.0526
<i>R</i> indices (all data)	0.0678	0.0621	0.0723	0.0490	0.0885
compound no.	6	7	8	9	10
formulas	C <sub>20</sub> H <sub>23</sub> ClN <sub>2</sub> O <sub>6</sub>	C <sub>40</sub> H <sub>46</sub> N <sub>4</sub> O <sub>8</sub> S	C <sub>20</sub> H <sub>24</sub> N <sub>2</sub> O <sub>6</sub> S	C <sub>20</sub> H <sub>25</sub> BF <sub>4</sub> N <sub>2</sub> O <sub>3</sub>	C <sub>20</sub> H <sub>23</sub> N <sub>3</sub> O <sub>5</sub>
CCDC no.	859879	859883	859881	859880	859882
mol wt	422.85	742.87	420.47	428.23	385.41
space group	<i>P</i> 2 <sub>1</sub> / <i>c</i>	<i>R</i> 3 <sub>2</sub>	<i>P</i> $\bar{1}$	<i>P</i> $\bar{1}$	<i>P</i> 2 <sub>1</sub> / <i>c</i>
<i>a</i> /Å	15.309(3)	15.094(8)	8.0024(6)	8.1285(5)	8.0447(12)
<i>b</i> /Å	8.9162(19)	15.094(8)	10.0959(8)	10.9801(7)	26.422(5)
<i>c</i> /Å	15.951(4)	48.91(5)	13.6380(10)	11.9948(7)	11.2878(18)
$\alpha$ /°	90.00	90.00	81.435(4)	96.789(4)	90.00
$\beta$ /°	110.878(13)	90.00	77.635(4)	95.608(4)	126.488(10)
$\gamma$ /°	90.00	120.00	70.938(4)	99.124(4)	90.00
<i>V</i> / Å <sup>3</sup>	2034.4(7)	9650(12)	1013.53(13)	1042.17(11)	1929.0(6)
density/Mg m <sup>-3</sup>	1.381	1.150	1.378	1.365	1.327
abs coeff/mm <sup>-1</sup>	0.227	0.127	0.200	0.114	0.097
<i>F</i> (000)	888	3546	3546	448	816
total no. of reflections	3675	4002	3546	3700	3215
reflections, <i>I</i> > 2σ( <i>I</i> )	1838	3309	2974	2552	1694
max $\theta$ /°	25.50	25.48	25.25	25.49	25.25
ranges ( <i>h</i> , <i>k</i> , <i>l</i> )	−18 ≤ <i>h</i> ≤ 17 −10 ≤ <i>k</i> ≤ 10 −19 ≤ <i>l</i> ≤ 18	−15 ≤ <i>h</i> ≤ 18 −18 ≤ <i>k</i> ≤ 18 −50 ≤ <i>l</i> ≤ 59	−9 ≤ <i>h</i> ≤ 9 −12 ≤ <i>k</i> ≤ 12 −16 ≤ <i>l</i> ≤ 14	−9 ≤ <i>h</i> ≤ 9 −13 ≤ <i>k</i> ≤ 11 −14 ≤ <i>l</i> ≤ 14	−9 ≤ <i>h</i> ≤ 8 −31 ≤ <i>k</i> ≤ 31 −13 ≤ <i>l</i> ≤ 11
complete to 2θ (%)	97.1	99.5	96.6	95.0	92.0
data/restraints/parameters	3675/0/279	4002/0/246	3546/0/277	3546/0/277	3215/0/266
GOF ( <i>F</i> <sup>2</sup> )	0.983	1.055	1.050	0.928	1.083
<i>R</i> indices [ <i>I</i> > 2σ( <i>I</i> )]	0.0730	0.0863	0.0457	0.0895	0.1774
<i>R</i> indices (all data)	0.1557	0.0741	0.0373	0.0635	0.1063

**Hlmbp-NO<sub>3</sub> (10).** A solution prepared from an equimolar amount (0.5 mmol) of Imbp (0.161 g) and HNO<sub>3</sub> was allowed to crystallize. After one week, colorless crystals were obtained. Yield, 95%. IR (cm<sup>-1</sup>): 3352 (s), 3125 (s), 3024 (s), 2914 (s), 1744 (w), 1615 (s), 1491 (s), 1439 (m), 1419 (m), 1384 (s), 1330 (s), 1300 (s), 1260 (s), 1226 (s), 1188 (s), 1096 (m), 1041 (m), 987 (w), 934 (w), 834 (m), 626 (w), 565 (w).

**Physical Measurements.** Infrared spectra (KBr pellets) of the solids were recorded on a Perkin-Elmer Spectrum One FT-IR

spectrophotometer in the spectral region 4000–400 cm<sup>-1</sup>. Thermogravimetric analysis (TGA) and differential scanning calorimetry (DSC) analyses were performed on a TA Instruments, SDT Q600 thermogravimetric analyzer, and Q20 differential scanning calorimeter respectively under an atmosphere of dry nitrogen from 25 to 500 °C with a heating rate of 5 °C.

**X-ray Crystallographic Studies.** Diffraction data for compounds 1–10 were collected at 296 K with MoK $\alpha$  radiation ( $\lambda$  = 0.71073 Å) using a Bruker Nonius SMART APEX CCD diffractometer equipped



with graphite monochromator and Apex CD camera. The SMART software was used for data collection and also for indexing the reflections and determining the unit cell parameters. Data reduction and cell refinement were performed using SAINT software and the space groups of these crystals were determined from systematic absences by XPREP and further justified by the refinement results. The structures were solved by direct methods and refined by full-matrix least-squares calculations using SHELXTL software. All the non-H atoms were refined in the anisotropic approximation against  $F^2$  of all reflections. The H-atoms attached to heteroatoms in these crystals were located in the difference Fourier synthesis maps and refined with isotropic displacement coefficients. Negligible absorption was found in each crystal. Crystal structure and details of the final refinement parameters of 1–10 are summarized in Table 3.

## ■ ASSOCIATED CONTENT

### Supporting Information

CIF of all the 10 structures 1–10; the powder XRD, TG analysis, FT-IR of all the salts,  $^1\text{H}$ NMR spectra of the salts. The materials are available free of charge via the Internet at <http://pubs.acs.org>.

## ■ AUTHOR INFORMATION

### Corresponding Author

\*E-mail: [juba@iitg.ernet.in](mailto:juba@iitg.ernet.in).

### Notes

The authors declare no competing financial interest.

## ■ ACKNOWLEDGMENTS

The authors are thankful to the Department of Science and Technology New-Delhi for XRD facility and financial assistance.

## ■ REFERENCES

- (1) (a) Steed, J. W.; Atwood, J. L. *Supramolecular Chemistry*; Wiley: Chichester, 2000. (b) Desiraju, G. R.; Sharma, C. V. K. In *The Crystal as a Supramolecular Entity*; Desiraju, G. R., Ed.; Wiley: Chichester, 1996, Chapter 2.
- (2) (a) Martinez-Manez, R.; Sancenon, F. *Chem. Rev.* **2003**, *103*, 4419. (b) An, H.; Bradshaw, J. S.; Izatt, R. M. *Chem. Rev.* **1992**, *92*, 543. (c) An, H.; Bradshaw, J. S.; Izatt, R. M.; Yan, Z. *Chem. Rev.* **1994**, *94*, 939. (d) Conn, M. M.; Rebek, J. Jr. *Chem. Rev.* **1997**, *97*, 1647.
- (3) (a) Desiraju, G. R. *Angew. Chem., Int. Ed.* **1995**, *34*, 2311. (b) Prins, L. J.; Reinhoudt, D. N.; Timmerman, P. *Angew. Chem., Int. Ed.* **2001**, *40*, 2382. (c) Endo, K.; Sawaki, T.; Koyanagi, M.; Kobayashi, K.; Masuda, H.; Aoyama, Y. *J. Am. Chem. Soc.* **1995**, *117*, 8341.
- (4) (a) Eddaoudi, M.; Moler, D. B.; Li, H.; Chen, B.; Reineke, T. M.; O'Keeffe, M.; Yaghi, O. M. *Acc. Chem. Res.* **2001**, *34*, 319. (b) Moulton, B.; Zaworotko, M. J. *Chem. Rev.* **2001**, *101*, 1629. (c) Evans, O. R.; Lin, W. *Acc. Chem. Res.* **2002**, *35*, 511. (d) Rao, C. N. R.; Natarajan, S.; Vaidhyanathan, R. *Angew. Chem., Int. Ed.* **2004**, *43*, 1466.
- (5) Thakuria, R.; Sarma, B.; Nangia, A. *Cryst. Growth Des.* **2008**, *8*, 1471.
- (6) Thallapally, P. K.; McGrail, P. B.; Dalgarno, S. J.; Atwood, J. L. *Cryst. Growth Des.* **2008**, *8*, 2090.
- (7) Skobridis, K.; Paraskevopoulos, G.; Theodorou, V.; Seichter, W.; Weber, E. *Cryst. Growth Des.* **2011**, *11*, 5275.
- (8) Brock, C. P.; Duncan, L. L. *Chem. Mater.* **1994**, *6*, 1307.
- (9) Sarma, R. J.; Baruah, J. B. *CrystEngComm* **2005**, *7*, 706.
- (10) (a) Sarma, R. J.; Baruah, J. B. *Cryst. Growth Des.* **2007**, *7*, 989. (b) Sarma, R. J.; Baruah, J. B. *Chem.—Eur. J.* **2006**, *12*, 4994. (c) Sarma, R. J.; Batsanov, A.; Baruah, J. B. *Acta Crystallogr.* **2005**, *C61*, 324.
- (11) (a) Tominaga, M.; Masu, H.; Azumaya, I. *CrystEngComm* **2011**, *13*, 5299. (b) Tominaga, M.; Katagiri, K.; Azumaya, I. *Cryst. Growth*

*Des.* **2009**, *9*, 3692. (c) Tominaga, M.; Masu, H.; Azumaya, I. *Cryst. Growth Des.* **2011**, *11*, 542.

(12) (a) Desiraju, G. R. *Acc. Chem. Res.* **1991**, *24*, 290. (b) Aitipamula, S.; Thallapally, P. K.; Thaimattam, R.; Jaskólski, M.; Desiraju, G. R. *Org. Lett.* **2002**, *4*, 921.

(13) Sarma, R. J.; Baruah, J. B. *Solid State Sci.* **2008**, *10*, 580.

(14) (a) Willans, C. E.; French, S.; Anderson, K. M.; Barbour, L. J.; Gertenbach, J.-A.; Lloyd, G. O.; Dyer, R. J.; Junk, P. C.; Steed, J. W. *Dalton Trans.* **2011**, *40*, 573. (b) du Plessis, M.; Barbour, L. J. *Dalton Trans.* **2012**, DOI: 10.1039/C1DT11564B.

(15) (a) Gandour, R. D.; Nabulsi, N. A. R.; Fronczek, F. R. *J. Am. Chem. Soc.* **1990**, *112*, 7816. (b) MacDonald, J. C.; Dorrestein, P. C.; Pilley, M. M. *Cryst. Growth Des.* **2001**, *1*, 29.

(16) Sarma, R. J.; Baruah, J. B. *Dyes Pigm.* **2004**, *61*, 39.

(17) (a) Orola, L.; Veidis, M. V.; Mutikainen, I.; Sarcevic, I. *Cryst. Growth Des.* **2011**, *11*, 4009. (b) Basavoju, S.; Boström, D.; Velaga, S. P. *Cryst. Growth Des.* **2006**, *6*, 2699. (c) Sethuraman, V.; Stanley, N.; Muthiah, P. T.; Sheldrick, W. S.; Winter, M.; Luger, P.; Weber, M. *Cryst. Growth Des.* **2003**, *3*, 823. (d) Wichmann, K. A.; Boyd, P. D. W.; Söhnel, T.; Allen, G. R.; Phillips, A. R. J.; Cooper, G. J. S. *Cryst. Growth Des.* **2007**, *7*, 1844.

(18) Bucar, D. K.; Henry, R. F.; Lou, X.; Borchardt, T. B.; Zhang, G. G. *Z. Chem. Commun.* **2007**, 525.

(19) Das, B.; Baruah, J. B. *J. Mol. Struct.* **2011**, *1001*, 134.

(20) Biradha, K.; Samai, S.; Maity, A. C.; Goswami, S. *Cryst. Growth Des.* **2010**, *10*, 937.

(21) (a) Haile, S. M.; Boyens, D. A.; Chisholm, C. R. I.; Merie, R. B. *Nature* **2001**, *400*, 910. (b) Chisholm, C. R. I.; Haile, S. M. *Solid State Ionics* **2000**, *229*, 136. (c) Lipkowski, J.; Baranowski, B.; Lunden, A. *Pol. J. Chem.* **1993**, *67*, 1867. (d) Haile, S. M. *Mater. Res. Soc. Symp. Proc.* **1999**, *547*, 315. (e) Bruce, P. G. *Dalton Trans.* **2006**, 1365.

(22) Braga, D.; Gandolfi, M.; Lusi, M.; Polito, M.; Rubini, K.; Grepioni, F. *Cryst. Growth Des.* **2007**, *7*, 919.

(23) (a) Braga, D.; Maini, L.; Polito, M.; Grepioni, F. *Struct. Bonding (Berlin)* **2004**, *111*, 1. (b) Braga, D.; D'Orta, E.; Grepioni, F.; Mota, F.; Novoa, J. J.; Rovira, C. *Chem.—Eur. J.* **2002**, *8*, 1173.

(24) Singh, U. P.; Kashyap, S.; Singh, H. J.; Butcher, R. J. *CrystEngComm* **2011**, *13*, 4110.

(25) (a) Holbrey, J. D.; Reichert, W. M.; Swatloski, R. P.; Broker, G. A.; Pitner, W. R.; Seddon, K. R.; Rogers, R. D. *Green Chem.* **2002**, *4*, 407. (b) Meszko, J.; Sikorski, A.; Huta, O. M.; Konitz, A.; Blazejowski, J. *Acta Crystallogr. C* **2002**, *58*, o669. (c) Funasaki, N.; Ishikawa, S.; Neya, S. *Bull. Chem. Soc. Jpn.* **2002**, *75*, 719. (d) Chang, H.-C.; Jiang, J.-C.; Tsai, W.-C.; Chen, G.-C.; Lin, S. H. *J. Phys. Chem. B* **2006**, *110*, 3302. (e) Bott, S. G.; Coleman, A. W.; Atwood, J. L. *J. Am. Chem. Soc.* **1988**, *110*, 610. (f) Blake, A. J.; Hubberstery, P.; Suksangpanya, U.; Wilson, C. L. *J. Chem. Soc., Dalton Trans.* **2000**, 3873.

(26) Kalita, D.; Baruah, J. B. *CrystEngComm* **2010**, *12*, 1562.